

Internal wave radiation from gravity current down a slope in a stratified fluid

J. Hazewinkel

Abstract

Experiments with gravity currents in stratified domains thus far ignored the possible radiation of internal waves. The main focus in those experiments has been on entrainment of ambient fluid into the current. Here, we focus on a dense current streaming down a gentle slope with very little entrainment of the ambient fluid. In a linearly stratified ambient, we observe internal waves being radiated from the nose of the dense current. The nose clearly slows down along the slope as its buoyancy difference with the ambient reduces. A simple model for the nose position in time compared well with the observations. In none of the experiments the internal waves emitted show a dominant frequency or wavelength. Rather, a whole spectrum of frequencies and wavelengths are found. We observe three different internal wave regimes, one in which the internal waves are observed close to the nose of the dense current, one in which the internal waves radiate freely out from the nose and one in which we do not find internal waves at all. In order to summarize the results we define an ambient (or bulk) Froude number, $Fr_b = U/(Nh_c)$, based on the stratification N , measured velocity U and the height of the current nose h_c . Using this Froude number we find the free internal waves for $1 < Fr_b < \approx 5$. This range indicates that internal wave emission from gravity currents is very dependent on ambient and local conditions of the flow. In the broader range of currents observed in the ocean it is expected that only a small part will meet these conditions.

1 Gravity currents

Gravity driven currents are naturally occurring flows that are found in atmosphere and ocean. In the atmospheric boundary layer, the so called katabatic winds are driven by dense air, formed by cooling, that flows downwards along the local topography. In the ocean there are currents that are similarly driven by their density anomaly. For example, at high latitudes brine rejection or extreme cooling at the surface increases the total density of the water column. In the Arctic, this dense water eventually spills in overflows through the Faroe Bank Channel and the Denmark Strait. These dense currents flow down the topography into the stratified ocean until they come to their level of neutral buoyancy.

The dynamics of these dense overflow currents has been considered in both theoretical and experimental studies. Some included the effect of rotation, others mainly considered the effect of stratification. Cenedese *et al.* (2004) and Adduce & Cenedese (submitted) included the effect of rotation in experiments with a dense current flowing down a slope in a homogeneous ambient. Different flow regimes were observed that varied from laminar flow, via a flow with roll waves, to a turbulent flow featuring breaking waves. Adduce & Cenedese (submitted) considered the resulting mixing in these different regimes. Mixing in dense currents in non-rotating but stratified environments has been quantified by Baines (2001) and Baines (2005) for slopes with several angles. Also in these studies different regimes were identified, a gravity current regime and a plume regime. In the gravity current regime a balance is

reached between the buoyancy force and drag, the current has a distinct upper interface. Mixing occurs only at this upper interface. In the plume regime the current is detached from the topography.

Not on a slope but on a flat bottom, Maxworthy *et al.* (2002) considered the propagation of a dense current in a stratified fluid, both experimentally and numerically. The dense fluid was initially behind a lock and was then released into the ambient stratified fluid. They used dye lines at regular heights to visualize the motion in the interior of the tank. When the gravity current moved at a velocity larger than the internal waves sustain (current faster than the fastest linear wave), the only waves seen were locked to the nose of the current. In this, so called, supercritical regime their Froude number, $Fr = U/(Nh)$ was larger than 0.318, U is the velocity of the nose of the dense current, h is the initial (before release) height of the dense fluid and N the buoyancy frequency. For lower, or sub critical, velocities the waves propagated out ahead of the nose of the current. However, due to their method of visualization, they could not obtain a more detailed picture of the internal waves, e.g. frequency or wavelength information, other than a sinusoidal raise and fall of the dye lines.

Internal waves, as found in linearly stratified fluids, are distinctly different from interfacial (internal) waves. Internal waves in linear stratifications will only propagate away from a disturbance if the frequency of the disturbance is less than the buoyancy frequency, $N = \sqrt{g/\bar{\rho}} \partial\rho'(z)/\partial z$. These internal waves will have the same frequency ω as the disturbance. Also, the energy will propagate under an angle θ with the vertical, or gravitational direction, following the dispersion relation $\omega = N \cos \theta$, Phillips (1977) and Mowbray & Rarity (1967). Surprising at first, the dispersion relation also predicts that the crest and troughs, i.e. the phase lines, travel perpendicular to the energy. Internal waves in the ocean are usually described as vertical modes. However, due to the above curious dispersion relation, near the generation areas this modal description breaks down while a ray-like description becomes more appropriate. Sources of internal wave rays in the ocean are predominantly the interaction of tides and topography as investigated in many studies. In the experimental study of Aguilar *et al.* (2006) internal waves were generated by dragging a sinusoidal 'topography' through a linearly stratified fluid. They observed different regimes in which waves could propagate freely into the ambient fluid or were evanescent and beyond which turbulence took over.

The motivation of this study came from the combination of the roll waves on the dense current observed by Cenedese *et al.* (2004) with the internal wave generation by a wave pattern by Aguilar *et al.* (2006). We intended to investigate whether the roll waves could be a source for internal wave generation. Since a dense current flowing down a slope can be seen as a disturbance of the stratified ambience, it can be expected that internal waves are found near a gravity current in a stratified fluid. The question is whether these waves can take out energy from the flow and transport it over a long distance. Also the investigation of a Froude number range for the existence of internal waves, as in previous studies, will be of interest.

The remainder of this paper is as follows. Section 2 describes the experimental apparatus used in this study. In Section 3 we present results from the experiments done followed by some analysis in Section 4. In Section 5 we summarize and discuss these results.

2 Method

To study the generation of internal waves by dense currents we use a perspex tank having dimensions $770 \times 210 \times 250$ cm (length, width, height). The well known double bucket method and salt are used to fill the tank with a stratification that linearly increases with depth. The water depth in the tank will be denoted by H . The maximum salinity, and thus the density, varied in each experiment. We present results from experiments where the maximum salinity varies between the salinity of the sea water from the tab, $\rho \approx 1.02\text{g/cm}^3$, to a very salty brine, $\rho \approx 1.1\text{g/cm}^3$. For the latter we use Morton's Kosher salt which does not contain supplements that affect the visibility of the water. After filling the tank, we

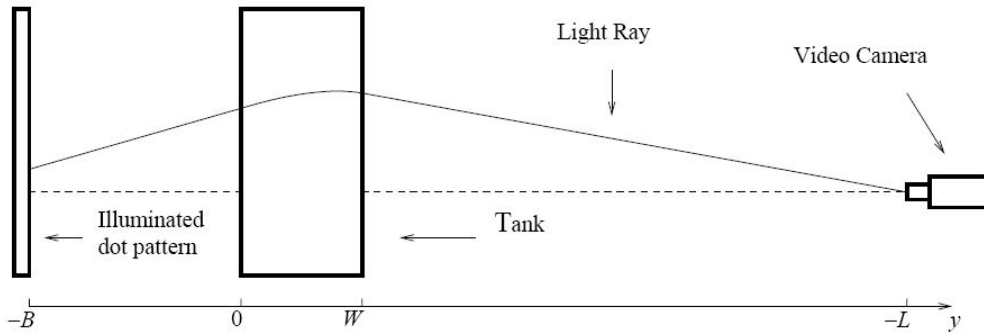


Fig. 1: Schematic of the experimental set up.

subtract samples from the fluid at several, typically six, vertical positions. The density of these samples is measured by a Anton Paar densimeter with a accuracy of 10^{-5} g/cm³.

In the earlier experiments, we would put the slope in after filling the tank. In this case, the slope runs from the upper left side of the tank under an angle α down to the right side of the tank. The source for the dense water is on top of the slope just below the surface. In the second set of experiments (presented in this report) the slope was already in the tank during the filling. In these experiments the lower side of the slope was at the bottom of the tank. In both cases the source, on top of the slope, was connected via a pump with a reservoir of water of density ρ_c , usually the same density as the fluid at the bottom of the tank. In some experiments this dense water was dyed.

To measure the motions in the fluid non-intrusively, we use the synthetic schlieren technique (Dalziel *et al.* (2000)). Synthetic schlieren measures the refractive index changes of a medium resulting from density perturbations. The principle is as follows. When a light-ray propagates through the fluid, the direction of propagation of this ray will be altered by the local value of the gradient of the index of refraction, see schematic in Figure 1. A random dot pattern on a light bank at $B = 0.2$ m behind the tank is monitored through the fluid. Density perturbations alter the refractive index and hence the direction of the light and are observed as apparent movement of the dots. Unfortunately, the refractive index of the air, between the tank and the point of observation, is also altered by unavoidable temperature fluctuations in the laboratory. This leads to some ‘thermal noise’ contaminating the observations and to minimize the effect we had curtains extending from the camera to the tank. To record the apparent movements, we use a Hitachi digital camera positioned at $L=3.2$ m from the tank. We try to zoom in as much as possible on a the region of interest in the tank. Also, we minimize the aperture as much as possible in order the reduce the errors resulting from light coming under an angle. As the buffer memory of the pc used is limited, we could only take 320 frame per experiment. However, we varied the amount of frames taken per second. Regarding an unperturbed reference image, the perturbed position of the dots is translated into corresponding density gradient variations. For this comparison and data processing we use the DigiFlow software. As we observe the changes in the density gradient field, the stronger the undisturbed gradient field is, the more the dots appear to move. For this reason the results of experiments with large N give better results. Also, as the current ‘lifts’ the whole stratification slightly in the vertical, we observe in most experiments a constant mean change in the stratification. Thereby, when the currents has passed the ambient fluid diffusive processes will smooth out the perturbed stratification. We will call this process re-stratification. We will present the observations as components of $\mathbf{b} = (b_x, b_z) = \nabla \rho' / (d\bar{\rho}/dz)$, i.e. the perturbation density gradient relative to the gradient of the unperturbed background stratification, $(d\bar{\rho}/dz)$.

Before the start of a typical experiment, we would leave the stratified tank undisturbed for some time after connecting the source and reservoir. We do this, to let re-stratification overcome small perturbations.

| Experiment | γ | N s^{-1} | ρ_c g/cm^3 | ρ_{bot} g/cm^3 | ρ_{top} g/cm^3 |
|-------------------------|----------|-----------------|----------------------|--------------------------|--------------------------|
| 030807 | 0.1 | 1.4 | 1.061 | 1.061 | 1.003 |
| 110807 | 0.05 | 1.7 | 1.071 | 1.073 | 1.009 |
| 130807 | 0.2 | 1.6 | 1.069 | 1.068 | 1.018 |
| 150807 | 0.1 | 0.9 | 1.022 | 1.022 | 1.004 |
| 160807 (default exp) | 0.1 | 1.6 | 1.069 | 1.062 | 1.016 |

Tab. 1: Parameters of the experiments presented

At the start of the experiment there would be no flow down the slope. Then, the pump will pump the dense water with a fixed flow rate Q , given in cm^3/s , into the source from where it enters the stratified fluid through a sponge. The pump was left running for the time that frames were taken.

3 Results

Several experiments with different slopes and stratifications were performed. We present results from the experiments listed in Table 1. In this table are listed the tangent of the slope $\gamma = \tan \alpha$, the buoyancy frequency N , the density of the current ρ_c and the density at the bottom/top of the tank $\rho_{bot,top}$. All experiments had a discharge $Q = 2.1 cm^3 s^{-1}$ and the slope ended at the bottom of the tank. We consider experiment 160807 as a default experiment with a slope of $\gamma = 0.1$ and a stratification $N = 1.6 s^{-1}$ and we will discuss the differences observed in the other experiments. Note that in these experiments the density of the current matches the density at the bottom of the tank.

3.1 Default experiment

Our default experiment has slope $\gamma = 0.1$ and a stratification $N = 1.6 s^{-1}$. The descent of the dense current is shown by three snapshots of b_x and b_z in Figures 2. The colour indicates the positive or negative gradients of the perturbation density field. We observe the descent of the dense current, shown by the darkest blue and red colour, Figures 2 a) and b), going over the slope in Figures 2 c) and d) and Figures 2 e) and f). When the nose is at mediate depth, Figures 2 c) and d), internal waves are radiated from the nose of the current. However, in the first snapshot, Figures 2 a) and b), the waves observed are close to the nose of the current, whereas in Figures 2 c) and d) the waves are found much further away. It is worth noticing that there is no clear defined angle under which the waves propagate. Finally, in the third snapshot, Figures 2 e) and f), the nose does not radiate any waves anymore although there is a remnant of the waves still visible from the nose of the dense current.

In order to find the position of the nose in time along the slope, we take a section parallel to the slope of b_x in time a few pixels above the slope. This section is shown in Figure 3. In the first 20 seconds of the experiment the nose is not in the camera field of view and no apparent movement is resolved. Figure 3 shows flat grey and changes gradation as soon as the nose comes in and shows clearly the position of the nose (vertical axis) in time (horizontal axis). Note that the velocity, or better displacement per time, of the current nose clearly decreases along the slope. Obtaining an accurate velocity proved to be

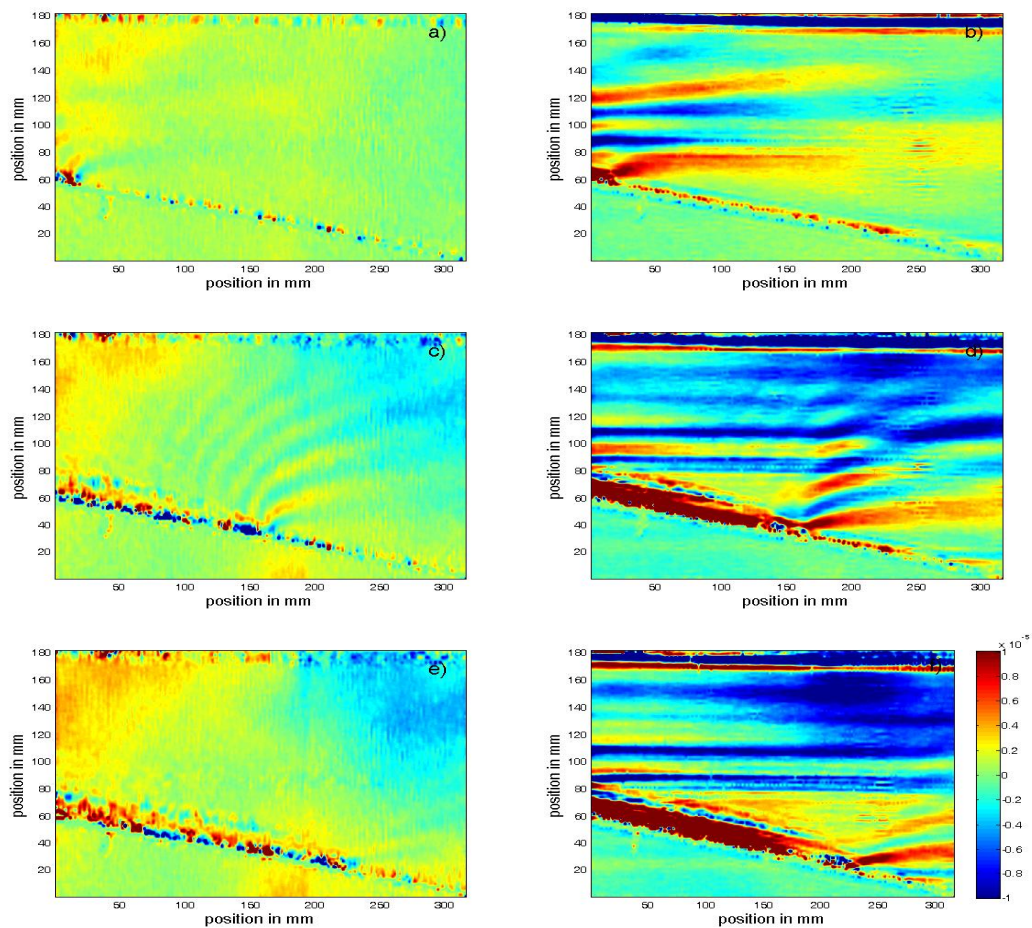


Fig. 2: Experiment 160807, three snapshots of b_x (left) and b_z (right), colour indicates value as in colour bar f). Shown are times $t=20$ s a) and b), 45 s c) and d) and 70 s e) and f) after the start of the experiment. Note that in the vertical gradient the re-stratification causes horizontal lines in the b_z data.

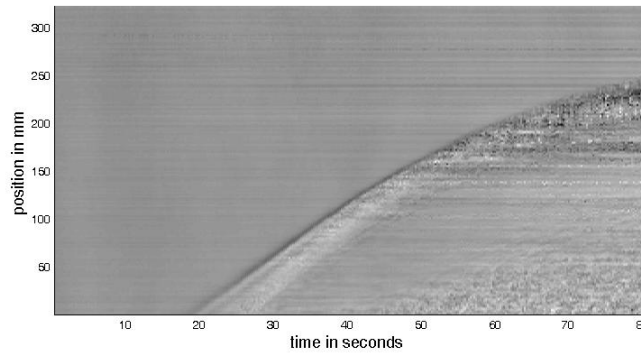


Fig. 3: Section of b_x of Experiment 160807 parallel to the slope in time. The colour changes indicates the position of the nose. Note the decrease in displacement in time

problematic as the data of the positions in time is not a smooth/differentiable curve. For later use, we take 10 cm bins and find the different times needed for the nose to travel them. From this we get average velocities along the slope.

3.2 Changing N

The results for the experiments with the same slope angle but different stratification, Experiments 030807 and 150807, show very similar qualitative results as observed in the default experiment. However, the waves are observed to radiate out from the nose starting from a point higher up on the slope. In Experiment 150807, after a short phase of bounded waves, the whole recorded descent of the current shows that the waves radiated are comparable with the default experiment as in Figures 2 c) and d). In experiment 030807 the waves disappear when the current slows down, similar as observed in Figures 2 e) and f). The position of the nose in time, in the same section just above the slope as in the default experiment, shows a lower velocities down slope. The positions in time of the current nose for both experiments are presented in Figure 8 as the noisy lines. Time is off set for clarity. Experiment 150807 (black line) shows very little slowdown while the velocity in experiment 030807 (green line) shows a stronger change in velocity as the nose flows down the slope.

3.3 Changing γ

We also carried out experiments with the same stratification as in the default experiment, i.e. $N = 1.6 \text{ s}^{-1}$ but in which the slope angle is changed. For a steeper slope, $\gamma = 0.2$, we observe the radiation of steep internal waves that are remain close to the nose of the current, as shown in Figure 4a). Down slope the current slows down and the internal wave field resembles that of the default experiment (Figures 2 c and d). The position of the nose is shown in Figure 8 by the blue line. In the experiment with a smaller slope, $\gamma = 0.05$, it is difficult to observe anything at all. First, the current is difficult to distinguish from the noise level and second, there are no internal waves generated by the dense current. Our algorithm to detect the position of the nose failed for this experiment and we do not plot it in Figure 8.

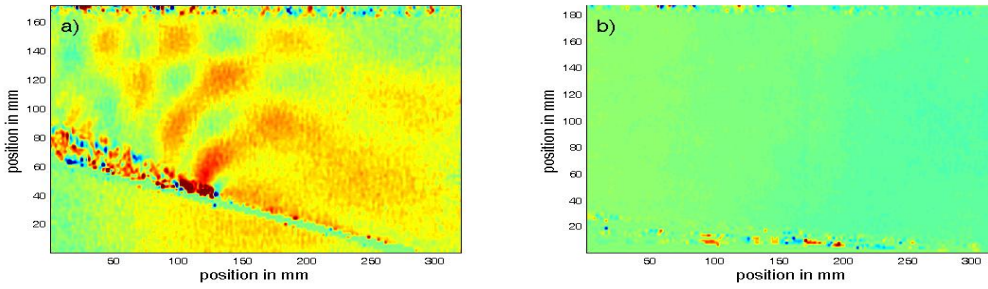


Fig. 4: b_x for two different slopes a) $\gamma = 0.2$ and b) $\gamma = 0.05$. Colour as in Figure 2

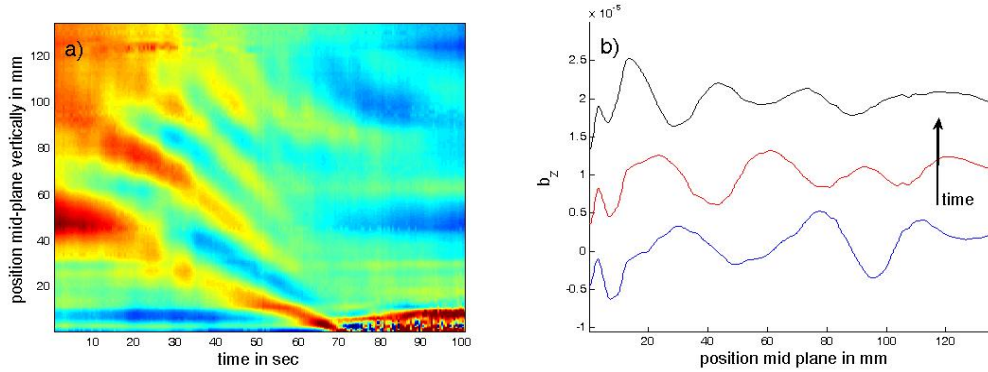


Fig. 5: Vertical section mid-slope of b_z of the default experiment. a) shows the amplitude of b_z along this line in the vertical vs time in the horizontal, colour as in Figure 2. b) shows three profiles from a).

4 Analysis

In our default experiment we observe that the radiated internal waves do not seem to have a clear angle of propagation or wave length. This observation seems generic for all experiments in which internal waves radiation is observed. This means that the following, although only presented for the default experiment, applies to the other experiments. In order to investigate whether there are dominant wave lengths or frequencies we take a vertical section mid-slope of b_z of the default experiment. This section runs from the slope up to the surface, vertical axis in Figure 5 a). Presented is the amplitude of b_z in colour and the development in time (horizontal axis). As this section is mid-slope the nose has not passed though it until $t = 70$ s, clearly seen in Figure 5 a). The wavelength in this section is observed to decrease as time increases, i.e. towards the nose, furthermore waves are absent after $t = 70$ s. Note that for $t > 70$ s some horizontal lines appear, this is the result of some re-stratification. We plot three individual sections at $t = 30, 40$ and 50 s in Figure 5b), to show that indeed no dominant wavelength is observed and that there is a clear decrease in wavelength in time. This result suggests that a whole range of wave lengths in generated by the dense current flowing down a slope in a stratified ambient.

In order to investigate whether there are dominant frequencies of the waves emitted by the dense current we take a second section. This section of b_z (default experiment), is taken parallel to the slope and 5 cm above it, Figure 6 a). The section is on the horizontal axis and the time on the vertical, the colour is the amplitude of b_z . Figure 6 a) shows a wave pattern moving obliquely in time (vertical axis), which is expected as we have a section parallel to the slope and the current nose is below it. Also, following the waves obliquely, the intensity of the colour, and thus b_z , diminishes along the slope. Time series of three points along the section, are shown in Figure 6 b). All three the sections show that a whole range

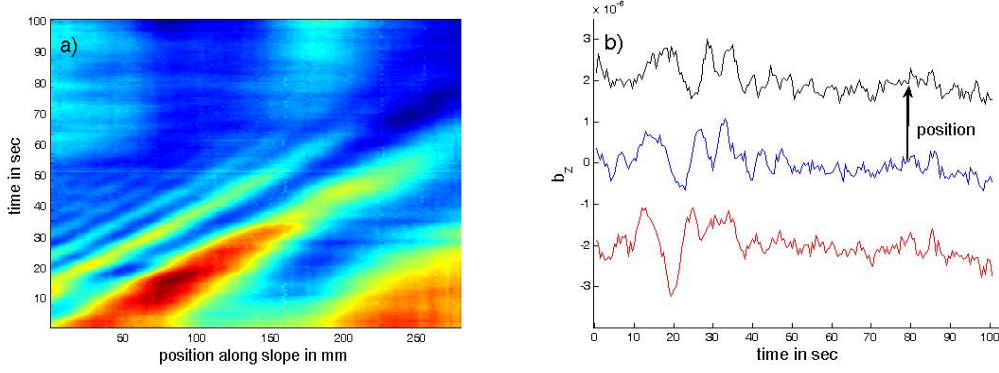


Fig. 6: Section parallel to the slope of b_z of the default experiment. a) shows the amplitude of b_z along this line in the horizontal vs time in the vertical, colour as in Figure 2 f). b) shows three profiles from a).

of frequencies is generated, note the decreasing period of the sinusoidal oscillations. This confirms the observation that a whole range of angles of propagation (dispersion relation) is found.

4.1 Simple model for nose position

The current nose is observed to slow down along the slope. The first cause for this is the increasing of the density of the surrounding fluid and the subsequent loss of buoyancy of the current. We will describe the nose speed in terms of the reduced gravity and current height h_c

$$U_f = \sqrt{g'(z)h_c \cos(\alpha)}, \quad g'(z) = g \frac{\rho_c - \rho(z)}{\bar{\rho}}, \quad (1)$$

based on Simpson & Britter (1979) but including the slope angle α . The vertical dependence of the reduced gravity $g'(z)$ is due to the decreasing difference in density between the local ambient fluid, $\rho(z)$, and the density of the current, ρ_c , as the current runs down the slope. The vertical coordinate is antiparallel with unprimed g , the acceleration due to gravity. We define $z = 0$ at the surface and $\rho(0) = \rho_{top}$. Similarly, at the bottom, $z = -H$, we will denote $\rho(-H) = \rho_{bot}$. We will assume that the stratification is linear over the tank depth H , i.e. $N^2 = g/\bar{\rho} (\rho_{bot} - \rho_{top})/H$ with $\bar{\rho}$ the characteristic density of water. This means that we can express the density as a function of the depth, i.e. $\rho(z) = \rho_{top} - N^2 \bar{\rho} z/g$. We also assume that the entrainment of ambient fluid into the dense current, which would cause a change in ρ_c , is negligible. The above assumptions combine in

$$U(z) = \sqrt{\left(\frac{g(\rho_c - \rho_{top})}{\bar{\rho}} + N^2 z \right) h_c \cos(\alpha)}. \quad (2)$$

This expression for $U(z)$ shows that for decreasing z the velocity decreases and comes to rest at the bottom, $z = -H$, for values of $\rho_c = \rho_{bot}$. From $U(z)$ we find an expression for $U(s)$, where $s = z \sin(\alpha)$ is the along slope coordinate. Integrating $U(s)$ in time results in the position on the slope of the current nose in time. Of the variables in Equation (2), only the current thickness $h_c = O(1mm)$ is unknown, for the others see Table 1. As an example we plot the position of the nose in experiment 160708 and two predictions in red for the positions of the nose based on $h_c = 1mm$ and $0.5mm$.

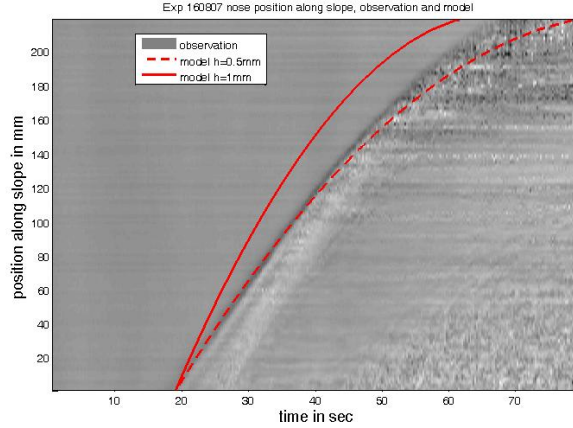


Fig. 7: Position of the nose in experiment 160708 and two predictions in red for the positions based on $h_c = 1\text{ mm}$ and 0.5 mm .

The two red curves show similar positions for the nose in time as the observations, suggesting that our estimate for the thickness of the current, $h_c = 1\text{ mm}$, is reasonable.

Similarly, we find that the positions of the nose for all the experiments listed in Table 1 can be predicted by Equation (2) by using a thickness of $h_c = 1\text{ mm}$ for the current. A combined plot of these nose positions (noisy lines) and theoretical curves (solid lines: $h_c=1\text{ mm}$ and dashed line $h_c=0.5\text{ mm}$) for the experiments listed in Table 1 are shown in Figure 8. Profiles of different experiments are offset for clarity. We observe that of the experiments with $\gamma = 0.1$ and varying N (black, red and green curves) only the prediction for experiment 030807 (green) is not accurate. Also for the nose position for the experiment with the steeper slope (experiment 130807, blue) the prediction works, remember that we did not have good data for experiment 110807. The fact that our observed and predicted positions of the nose on the slope agree so well, suggests that little to no loss of velocity is caused by internal wave radiation. After all, if there would be any loss this would show up as a discrepancy from velocity loss due to buoyancy effects, i.e. our prediction.

As our observed nose velocities have values that are of order $\sqrt{g'(z)h_c \cos(\alpha)}$, the local Froude number will always be

$$Fr = \frac{U}{\sqrt{g'(z)h_c \cos(\alpha)}} \approx 1. \quad (3)$$

Hence, the different regimes observed can not be related to the local Froude number. However, we can make that distinction when we consider a bulk $Fr_b = U/(Nh_c)$, similar to e.g. Aguilar & Sutherland (2006) and Maxworthy *et al.* (2002). It is worth remarking that the relevant height is h_c , since the slope or height of the free surface could in principle be extended without influencing the internal waves regimes. The height of the current however, plays a crucial role in determining the velocity of the nose and thus the radiation of waves. This definition of Fr_b requires an estimate for the velocity of the nose. We estimate these velocities by taking the displacements of the nose over several seconds and subsequently calculate the average velocities. Assuming that $h_c = 1\text{ mm}$ we find that the Fr_b varies from 6 to 1, as shown in Table 2. Although it seems that bounded waves are found from $Fr_b > 4.3$ in experiment 160807 we observe radiating waves in experiment 150807 with a $Fr_b=5$. This indicates that perhaps our definition of bounded and radiating waves is not correct. Alternatively it might be argued that the thickness of the current is assumed to be the same in all experiments, i.e. 1 mm , and that this thickness could vary between experiment and change the Froude numbers. In any case, Table 2 indicates

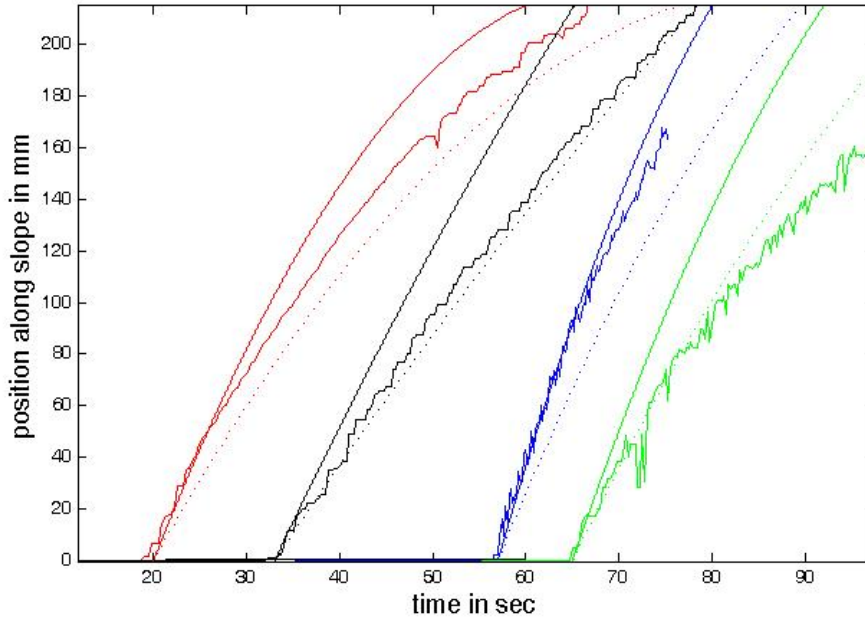


Fig. 8: Comparison between observed position of current nose along the slope (noisy line) and the model (solid ($h_c = 1$ mm) and dashed lines ($h_c = 0.5$ mm)). For clarity the profiles are set off. Colour correspond to Experiment 030807 (green), 130807 (blue), 150807 (black) and 160807 (red).

that a dense current flowing down a slope in a stratified ambience radiates internal waves $Fr_b < 5$.

5 Discussion and Conclusions

In this report experiments are presented investigating internal wave generation from a gravity current. We conclusively show that the nose of a gravity current does emit internal waves. Originally, we intended to investigate whether or not the roll waves, observed by Cenedese *et al.* (2004), would be a suitable generating mechanism for internal waves comparable with the generation of internal wave by a sinusoidal topography (Aguilar & Sutherland, 2006). However, the presented experiments were not in the roll wave regime. For the highest Froude numbers investigated, the internal waves were bounded and the current was still in the laminar regime. This suggests that the roll wave regime might be outside the internal wave radiation regime and if occurring will not radiate internal waves. However, at the lower Froude numbers we did observe internal waves radiating from the nose of the dense current and found a clear dependence of the internal waves radiation on the nose velocity. The nose velocity was well described by the local gravity wave velocity and consequently depends on the unknown/unmeasurable height of the current. Using a reasonable guess for the current height made it possible to compare the measured and predicted position of the nose on the slope in time with good agreement for h_c between 1 and 0.5 mm.

We thank Keith Bradley for his expertise in the laboratory, Steve Thorpe for useful suggestions and the GFD staff and fellows for the summer. JH obtained a GFD Fellowship.

| Experiment | displacement (mm) | Δt (s) | average velocity (mm/s) | Fr_b | regime |
|------------|-------------------|----------------|-------------------------|--------|------------------|
| 030807 | 80 | 15 | 5.3 | 3.8 | radiating waves |
| 030807 | 28 | 20 | 1.4 | 1 | horizontal waves |
| 110807 | - | - | <0.2 | <0.1 | no waves |
| 130807 | 36 | 5 | 7.2 | 4.5 | bounded waves |
| 150807 | 55 | 10 | 5.5 | 6 | bounded waves |
| 150807 | 45 | 10 | 4.5 | 5 | radiating waves |
| 160807 | 34.5 | 5 | 6.9 | 4.3 | bounded waves |
| 160807 | 39 | 10 | 3.9 | 2.4 | radiating waves |
| 160807 | 14 | 5 | 1.8 | 1.1 | horizontal waves |

Tab. 2: Estimated values for Fr_b and the observed internal waves

References

- ADDUCE, C. & CENEDESE, C. submitted Mixing in a density driven current flowing down a slope in a rotating fluid. *Journal of Fluid Mechanics* .
- AGUILAR, D. A. & SUTHERLAND, B. R. 2006 Internal wave generation from rough topography. *Physics of Fluids* **18**, online.
- AGUILAR, D. A., SUTHERLAND, B. R. & MURAKI, D. J. 2006 Laboratory generation of internal waves from sinusoidal topography. *Deep-Sea research II* **53**, 96–115.
- BAINES, P. G. 2001 Mixing in flows down gentle slopes into stratified environments. *Journal of Fluid Mechanics* **443**, 237–270.
- BAINES, P. G. 2005 Mixing regimes for the flow of dense fluid down slopes into stratified environments. *Journal of Fluid Mechanics* **538**, 245–267.
- CENEDESE, C., WHITEHEAD, J. A., ASCARELLI, T. A. & OHIWA, M. 2004 A dense current flowing down a sloping bottom in a rotating fluid. *Journal of Physical Oceanography* **34**, 188–203.
- DALZIEL, S. B., HUGHES, G. O. & SUTHERLAND, B. R. 2000 Whole field density measurements by 'synthetic schlieren'. *Experiments in Fluids* **28**, 322–335.
- MAXWORTHY, T., LEILICH, J., SIMPSON, J. E. & MEIBURG, E. H. 2002 The propagation of a gravity current into a linearly stratified fluid. *Journal of Fluid Mechanics* **453**, 371–394.
- MOWBRAY, D. E. & RARITY, B. S. H. 1967 A theoretical and experimental investigation of the phase configuration of internal waves of small amplitude in a density stratified liquid. *Journal of Fluid Mechanics* **28**, 1–16.
- PHILLIPS, O. M. 1977 *The Dynamics of the Upper Ocean, 2nd ed.*. Cambridge University Press.
- SIMPSON, J. E. & BRITTER, R. E. 1979 The dynamics of the head of a gravity current advancing over a horizontal surface. *Journal of Fluid Mechanics* **94**, 477–495.